23rd ABCM International Congress of Mechanical Engineering
December 6-11, 2015, Rio de Janeiro, RJ, Brazil

NUMERICAL ANALYSIS OF THE BLANKING PROCESS OF INCONEL 718 SHEETS FOR NUCLEAR FUEL SPACER GRIDS

Rafael Oliveira Santos
Luciano Pessanha Moreira
Graduate Program on Mechanical Engineering, Universidade Federal Fluminense, Av. dos Trabalhadores, 420, CEP 27255-125, Volta Redonda – RJ, Brazil.
rafaeloliveirasantos@id.uff.br, luciano.moreira@metal.eeimvr.uff.br

Marcelo Costa Cardoso
Graduate Program on Metallurgical Engineering, Universidade Federal Fluminense, Av. dos Trabalhadores, 420, CEP 27255-125, Volta Redonda – RJ, Brazil.
marcelocardoso@metal.eeimvr.uff.br

Abstract. *Spacer grid assembly supporting the nuclear fuel rods is an important concern in the design of structural components of a Pressurized Water Reactor (PWR). The spacer grid is composed by springs and dimples which are formed from a strip sheet by means of blanking and stamping process. In particular, the blanking process may produce forming defects such as scratches, cracks and cavities. These defects are typically induced by the formation of burrs and slivers resulting from the shearing process owing to the clearance between the punch and the die or else tooling wear. In this work, blanking process parameters, namely, the punch velocity and punch-die clearance, as well as the tooling geometry are numerically evaluated by means of a plane-strain finite element model in order to evaluate the quality of the sheared edges of Inconel 718 strips.*

Keywords: *Spacer grids, Blanking process, Inconel 718, Damage, Finite Element Modelling.*

1. INTRODUCTION

The spacer grids of nuclear fuel assembly are structural components with reticulated geometry that can be made of Inconel 718. The spacer grids are used to maintain adequate spacing between the fuel rods, to give stiffness for the fuel assembly, to improve the refrigerant mixing and to prevent damage during the nuclear fuel operation. The strips of Inconel 718, which compose a spacer grid, can be formed by a blanking process. Blanking process is a shearing process, in which there are usually four characteristic regions in the cutting edge. Figure 1 depicts a sheet blanking process wherein the workpiece material is placed between a die and a holder while it is deformed by the punch displacement. The process continues until the fracture, creating the four regions, namely, rollover, burnish zone, fracture zone and burr, as indicated in Fig.1(b). An ideal cutting produces only the burnish zone, without rollover, fracture zone or burr. However, in a real process all regions are commonly observed, due to elastic and plastic strains (Wang, *et al.*, 2012). Besides the material parameters, the blanking involves several process parameters, for example, the blanking clearance, punch velocity, sheet thickness and the tooling angles (Poizat, *et al.*, 2005).

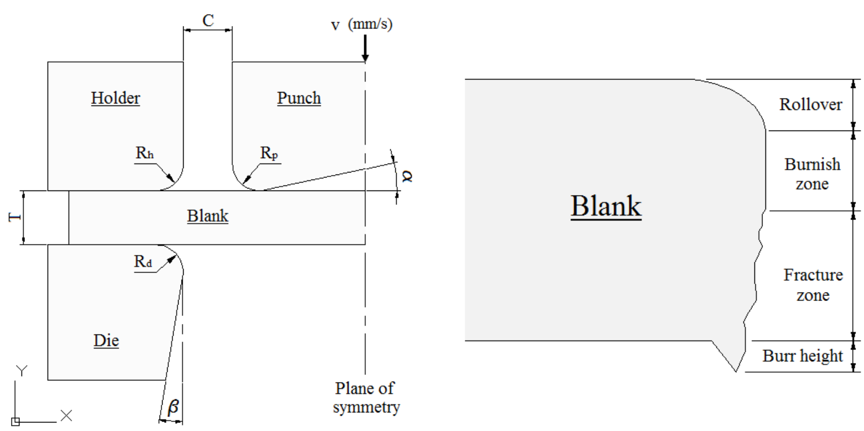

(a) (b)

Figure 1. Sheet blank process: (a) tooling parameters and (b) sheared edge.

In this work, the blanking process of the Inconel 718 strips used in nuclear spacer grids is numerically investigated in order to evaluate the influence of both process and tooling parameters upon the sheared edge quality and punch load. The numerical simulations were performed with the commercially available Finite Element code ABAQUS/Explicit by means of a plane-strain model with linear isotropic elasticity along and associated flow rule under isotropic work-hardening assumption.

2. MATERIAL AND METHODS

The experimentally investigated material is an Inconel 718 delivered by “Indústrias Nucleares do Brasil (INB)” as cold rolled thin sheet in the annealed state condition with a nominal thickness of 0.36 mm. The chemical composition of Inconel 718 provided by the supplier is listed in Tab. 1.

Table 1. Inconel 718 chemical composition (% weight)

Ni	Cr	Nb	Mo	Ti	Al	Fe	Cu	Si	Mn	C	Co	Ta	S	B	P
54.07	18.34	4.91	2.98	0.98	0.55	18.05	0.02	0.08	0.04	0.04	0.02	0.01	0.0005	0.003	0.006

2.1 Experimental procedure

The mechanical properties of the Inconel 718 sheet were evaluated by means of uniaxial tensile testing using an electromechanical universal machine EMIC DL 2000 20 KN load capacity equipped with a 50 mm gauge extensometer. The specimen shape and dimensions for uniaxial tensile testing are shown in Fig.2. The uniaxial tensile tests were conducted at room temperature using a constant cross-head speed of 1 mm/min. In order to ensure testing repeatability, at least three specimens were tested.

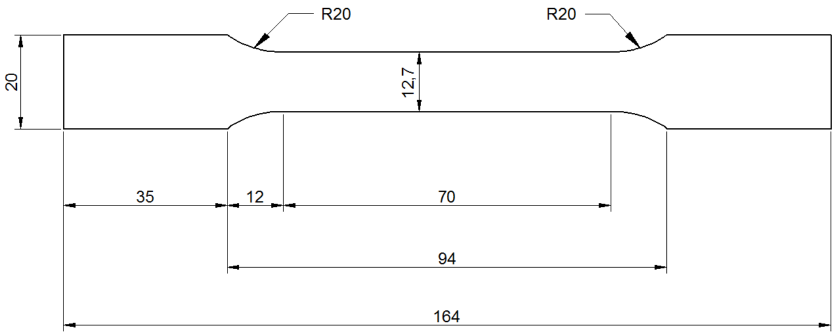

Figure 2. Uniaxial tensile specimen dimensions (mm).

2.2 Plastic behavior

In this work, the phenomenological equation of Johnson-Cook is used to model the Inconel 718 sheet plastic behavior. The Johnson-Cook equation is commonly used to describe the plastic material behavior at high strain-rate and elevated temperatures conditions as, for instance, in crash and machining finite element simulations (Wang, *et al*., 2013 and Uhlmann, *et al*., 2013). The Johnson-Cook model is available in the ABAQUS/Explicit commercial finite element code (ABAQUS, 2009) and is defined as:

$$\sigma_y = [A + B(\varepsilon^p)^n]\left(1 + C\ln\frac{\dot{\varepsilon}^p}{\dot{\varepsilon}_o}\right)\left[1 - \left(\frac{T - T_r}{T_m - T_r}\right)^m\right] \tag{1}$$

In the Johnson-Cook equation, the term in the first bracket describes the material dependence on strain-hardening while the second term describes the instantaneous strain-rate sensitivity and the third term represents the stress temperature dependence. In Eq. (1), T_r is a reference temperature whereas T_m is the melting temperature of the material. The set of material parameters of the Johnson-Cook equation are given by A, B, C, n and m (Johnson and Cook, 1985). The parameter C controlling the viscoplastic hardening can be determined by inverse modeling based on the field information determined from the dynamic testing (Kajberg and Wikman, 2007). Similarly, the thermal softening parameter m can be determined from some tests performed at different temperatures (Milani, *et al*., 2009).

Neglecting the strain-rate dependence and temperature effects, Eq. (1) reduces to the work-hardening equation proposed by Ludwik, that is,

$$\sigma_y = A + B(\varepsilon^p)^n \tag{2}$$

For metal forming processes where this simplification is acceptable, the simulation results from both Johnson-Cook and Ludwik equations provided close predictions (Pantalé and Gueye, 2013). This assumption is adopted hereafter to describe the Inconel 718 behavior during the blanking process.

2.3 Damage and rupture modelling

The continuum damage mechanics describes the progressive workpiece failure due to the material degradation (Lemaitre, 1996). Johnson and Cook (1985) proposed a ductile failure criterion based on the continuum damage parameter D ($0 \leq D \leq 1$) as a function of the accumulated equivalent plastic strain defined as:

$$D = \sum \frac{\Delta \bar{\varepsilon}^p}{\varepsilon_r} \tag{3}$$

With,

$$\varepsilon_r = [d_1 + d_2 \exp(d_3 \Sigma)] \left(1 + d_4 \ln \frac{\dot{\bar{\varepsilon}}^p}{\dot{\varepsilon}_o}\right) \left[1 + d_5 \left(\frac{T - T_r}{T_m - T_r}\right)\right] \tag{4}$$

In which d_i (i =1, 5) are material parameters while $\Sigma = \sigma_H/\sigma_{vM}$ is the stress triaxiality factor defined by the ratio between the hydrostatic stress component, $\sigma_H = \sigma_{ii}/3$, σ_{ii} is the trace of the Cauchy stress tensor $\boldsymbol{\sigma}$, and the equivalent von Mises stress, σ_{vM}.

Pantalé, *et al.*, (2004) have proposed in their contribution to identify the material parameters d_1, d_2, and d_3, in Eq. (4), from tensile tests using notched specimens with different radii. The constants d_4 and d_5 are determined by tensile and torsion tests. However, it is difficult to apply this methodology to very thin sheets which are prone to buckling. Furthermore, it is necessary to use a digital correlation image technique to measure in-situ the displacement fields in the specimen. Thus, neglecting the strain-rate dependence and the temperature effects, Eq. (4) can be rewritten as:

$$\varepsilon_r = d_1 + d_2 \exp(d_3 \Sigma) \tag{5}$$

In this work, the material parameters in Eq. (5) were determined from finite element simulations of the experimental conditions adopted in the uniaxial tensile testing of the Inconel 718 sheet. In order to simplify these numerical analyses, a single 3D solid element with only one integration point was adopted along with 1/8 symmetry boundary conditions, schematically shown in Fig. 3(a). In ABAQUS/Explicit finite element code to model the progressive damage which will cause the failure in ductile metals, one needs to specify: (1) the damage initiation criterion; (2) the damage evolution and (3) the element removal. Eq. (5) defines the damage initiation criterion while the damage evolution can be specified either as a function of the fracture energy or the elongation after the maximum load (post-necking hardening behavior). From the experimental load-elongation curves, it is observed a sudden fracture behavior of the Inconel 718 sheet and, thus, a linear damage evolution was defined based on the average elongation values obtained between the maximum load and failure. Finally, the element is removed from the mesh when the damage parameter reaches its maximum value and the stresses are set to zero as depicted schematically in Fig. 3(b).

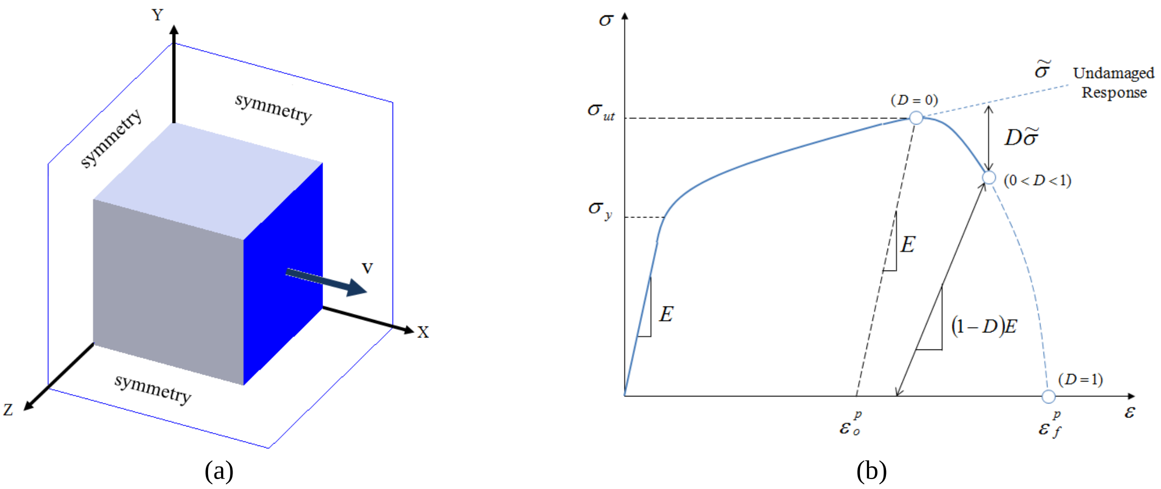

Figure 3. Identification methodology to determine the parameters of the Johnson-Cook (1985) ductile failure model: (a) 3D element with symmetry boundary conditions (b) stress-strain curve with progressive damage (ABAQUS, 2009).

3. FINITE ELEMENT ANALYSIS

3.1 Blanking process

The blanking is a complex process of plastic shearing and fracture in which the material at the edge is likely to become hardened locally (Marciniak, *et al*., 2002). The major variables in this process are as follows: the punch force, the punch velocity, the surface conditions and the tooling materials; the lubrication conditions and the amount of clearance between the punch and die.

In order to investigate the clearance effects on the wear tooling of the sheet blanking of the AISI 4304 2 mm thick, Ko and Kim (2000) tested clearances with 5, 10 and 20 % of the nominal sheet thickness. For the blanking of copper, Poizat, *et al.*, (2005) adopted a clearance of 8 % of the sheet thickness. To analyze the shearing process of Zircalloy sheets 0.58 mm thick used in nuclear fuel spacer grids, Wang, *et al*., (2012) adopted clearances values of 0.01 mm and 0.02 mm. In the present work, these values are adopted for the punch-die gap of the blanking process of Inconel 718. Moreover, the values of 100 and 200 mm/min were adopted to investigate the influence of the punch velocity. According to Fig. 1(a), the angle α between the punch and blank surface varies in the range of 0 and 12 degrees while the angle β at the die wall varies between 0 and 3 degrees (Boljanovic, 2004). Thus, assuming the tooling radii equal to 0.01 mm, see Fig. 1(a), along with the selected punch-die clearances C-values (0.01 and 0.02 mm), the punch velocities (100 and 200 mm/min) and the different tooling angles, a total of 16 combinations were simulated as listed in Tab. 2.

Table 2. Different setups for the numerical simulation of the blanking process of the Inconel 718 sheet.

Case number	v(mm/min)		C (μm)		α (degrees)		β (degrees)	
	100	200	10	20	0	12	0	3
11000	●		●		●		●	
12000	●			●	●		●	
11120	●		●			●	●	
12120	●			●		●	●	
11003	●		●		●			●
12003	●			●	●			●
11123	●		●			●		●
12123	●			●		●		●
21000		●	●		●		●	
22000		●		●	●		●	
21120		●	●			●	●	
22120		●		●		●	●	
21003		●	●		●			●
22003		●		●	●			●
21123		●	●			●		●
22123		●		●		●		●

3.2 Finite element model

A 2D plane-strain model was built to simulate the blanking process of Inconel 718 sheets. The elastic behavior of the blank is defined by Hooke's law with Young modulus E equal to 197,689 MPa and Poisson's ratio ν equal to 0.29. The plastic behavior is described by Ludwik's work-hardening equation, Eq. (2), which is fitted to the experimental uniaxial tensile data. Isotropic work-hardening and associated flow rule are adopted along with von Mises yield criterion. The blanking tools were assumed as rigid and described by means of analytical rigid surfaces. Coulomb law was assumed between the tooling and blank contact surfaces with a friction coefficient equal to 0.3. The blank is meshed with 16,384 linear quadrilateral plane-strain elements with reduced integration, CPE4R according to ABAQUS/Explicit terminology. Fig. 4 shows the adopted mesh to represent the cutting region, allowing to refine only the region of interest (Anjos and Moreira, 2014), where it is worth to observe structured mesh in which the smallest element size is equal to 1.2 micrometers whereas the largest element size is equal to 48 micrometers. In order to avoid excessively element distortion, Arbitrary Lagrangian-Eulerian (ALE) adaptive meshing was activated. The numerical simulations were run in a dual-processor Intel Xeon X5690 workstation with 3.47 GHz and 24 cores with ABAQUS/Explicit academic research version 6-9.

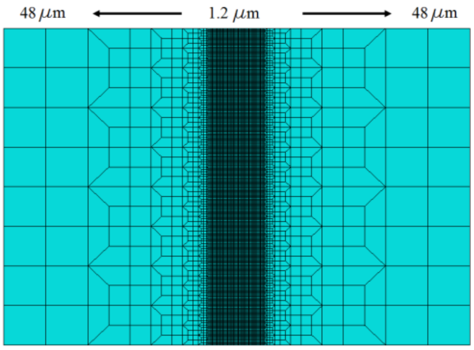

Figure 4. Adopted finite element mesh for the blanking process of the Inconel 718 sheet.

4. RESULTS AND DISCUSSION

4.1 Mechanical properties

From the uniaxial tensile tests performed at room temperature conditions under a cross-head speed of 1 mm/min, which corresponds to a low strain-rate ~ 3 x 10^{-4} s^{-1}, the Inconel 718 showed a good ductility along with a high work-hardening rate as shown in Fig. 5(a). However, the Inconel 718 thin sheet presented an abrupt fracture without any apparent localized necking, as shown in detail in Fig. 5(b). The obtained engineering stress-strain curve has similar values with the experimental values of the Inconel 718 1.6 mm thick sheets investigated by Alexopoulos, *et al.* (2014). The parameters of Ludwik's work-hardening equation fitted from the uniaxial tensile data are listed in Tab. 2.

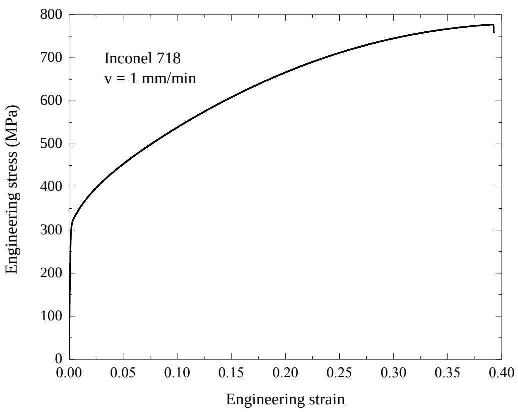

(a)

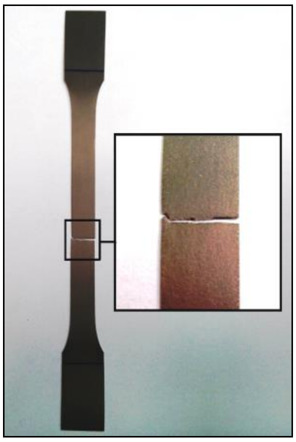

(b)

Figure 5. Experimental uniaxial tensile test results obtained for the Inconel 718 sheet: (a) engineering stress-strain curve and (b) detail of a fractured specimen.

Table 2. Inconel 718 plastic parameters fitted from uniaxial tensile data.

A (MPa)	B (MPa)	n
301.97	1,918.83	0.7958

4.2 Identification of the damage parameters

Figure 6 compares the predictions of the uniaxial true stress-strain curve determined with some set values adopted for the Johnson-Cook damage parameters, Eq. (5), with the experimental curve determined for the Inconel 718 sheet. Table 3 presents the best fitting found for the damage parameters as well as the parameters for the element deletion, namely, effective plastic displacement at failure (u^f) and maximum degradation (D_{max}).

Table 3. Material parameters of the ductile damage model.

d_1	d_2	d_3	u^f (mm)	D_{max}
0.107	0.156	-1	0.101	0.03975

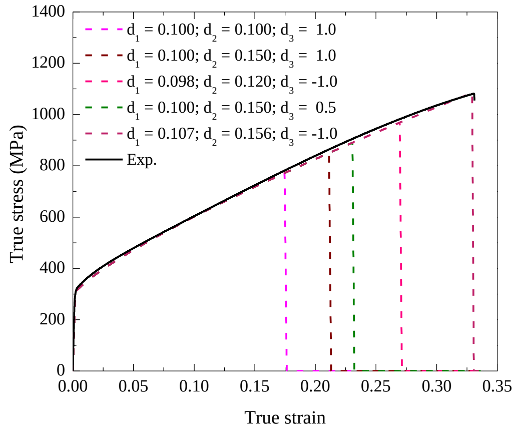

Figure 6. Calibration of Johnson-Cook damage parameters by means of comparisons between numerical predictions and the experimental true stress-strain curve determined from uniaxial tensile test of the Inconel 718 sheet.

4.3 Analysis of process and tooling parameters

Figure 7 shows the predicted punch force as a function of the normalized punch displacement with respect to initial blank thickness determined from proposed arrangements defined in Table 2 which are discussed with respect to the angle α between the punch and blank surface (0 and 12 degrees) and grouped in two sets. The first set is defined as a function of the tooling clearance, represented by dashed lines ($C = 0.01$ mm) while the second is given by continuous lines ($C = 0.02$ mm) together with two combinations of the angle β at the die wall (0 and 3 degrees) and two punch velocities (100 and 200 mm/min). Firstly, the punch force decreases with an increase of the angle α between the punch and blank surface which is attributed to the decrease of the contact area. In addition, the normalized punch displacement forces indicate that the blanking process is completed between ~ 25 and 35 % of the initial Inconel 718 blank thickness. It is also observed that the tooling clearance influenced the punch displacement evolution up to fracture which is more abrupt for a small clearance $C = 0.01$ mm (dashed lines) in comparison to a larger clearance value $C = 0.02$ mm (continuous lines).

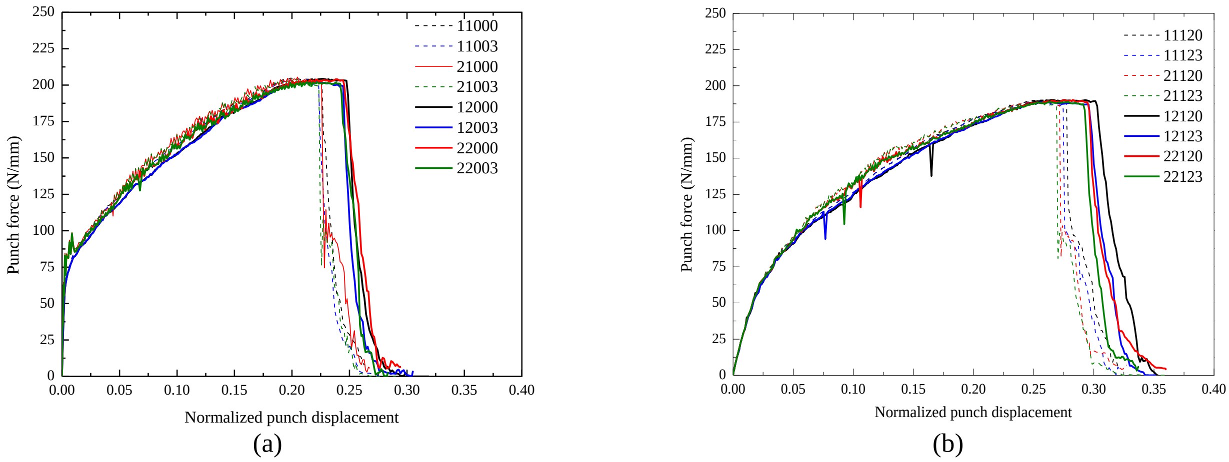

Figure 7. Predicted punch force in the blanking process of Inconel 718: (a) α = 0 and (b) α = 12 degrees.

Bearing in mind an ideal blanking process free of any cutting defects which would give a largest burnish area, Table 4 summarizes the numerical predictions determined from the 16 combinations defined in Table 2 in terms of the percent values of burnish, rollover and fracture zones, which summation gives the initial blank thickness (0.36 mm), together with the burr height (μm) and the maximum punch load. Based upon the sheared edge quality criterion with the largest burnish area zone, the simulated cases in Table 4 were ranked between the best process and tooling parameters set defined by v = 100 mm/min, $C = 0.02$ mm, $\alpha = 12$ degrees and $\beta = 3$ degrees and the worst parameters combination which is given by v = 200 mm/min, $C = 0.01$ mm, $\alpha = 0$ degrees and $\beta = 3$ degrees. Figure 8 shows the corresponding predicted sheared edge profiles along with intermediate cases (11120 and 12000) where one can observe the deformed blank mesh indicating the cutting zones. In fact, these sheared edge predictions are highly affected by the mesh density as well as the element deletion procedure mainly near to the burr zone formation where the elements are too distorted.

Table 4. Ranking of the proposed numerical simulations for the blanking process of Inconel 718 strips.

Ranking	Case number	Burnish (%)	Rollover (%)	Fracture (%)	Burr (μm)	Force (N/mm)
1st	12123	21.5	9.6	68.9	3.54	188
2nd	12120	20.5	11.8	67.7	1.62	190
3rd	11123	18.8	11.6	69.6	4.96	189
4th	22123	18.6	11.8	69.6	1.78	188
5th	11120	18.2	11.3	70.5	3.43	190
6th	22120	17.8	11.8	70.4	1.13	190
7h	21120	17.5	10.7	71.8	2.29	189
8th	21123	17.5	10.6	71.9	4.02	187
9th	12000	14.6	12.7	72.8	3.83	204
10th	21000	13.6	11.7	74.8	4.37	203
11th	22003	13.2	13.1	73.7	3.35	202
12th	22000	13.1	13.0	73.9	3.48	204
13th	12003	12.7	13.8	73.5	2.35	201
14th	11000	12.7	12.4	74.9	2.30	204
15th	11003	12.5	11.6	75.9	8.92	204
16th	21003	11.4	12.3	76.3	5.56	204

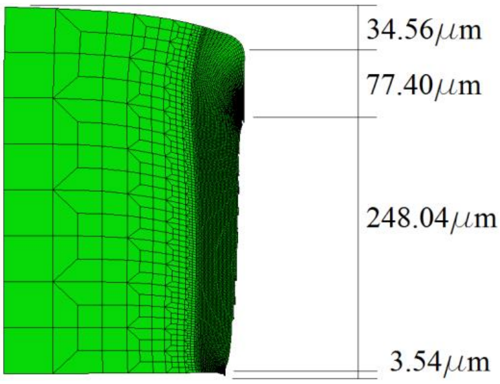

(a) 12123

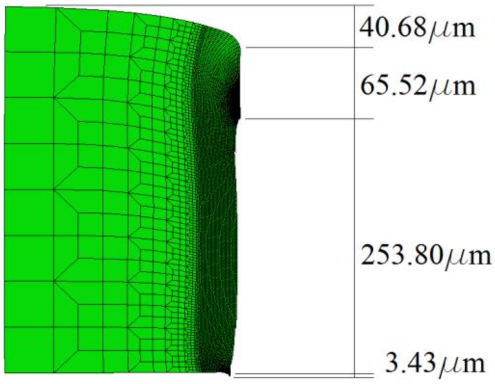

(b)11120

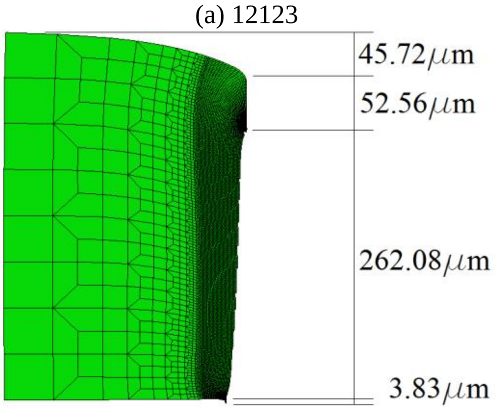

(c)12000

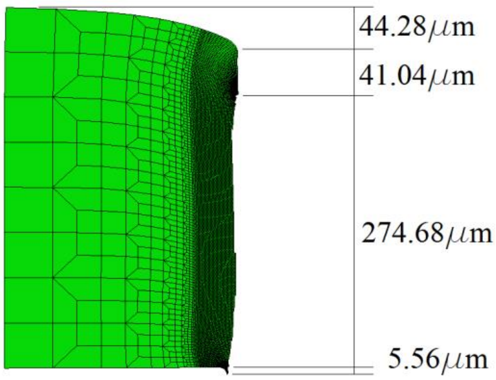

(d)21003

Figure 8. Sheared edge profiles predicted by finite element simulations of the blanking process of Inconel 718 strips: (a) 12123, (b) 11120, (c) 12000 and (d) 21003 cases defined by the process and tooling parameters listed in Table 2.

5. CONCLUSION

In this work, the mechanical properties of an Inconel 718 strip 0.36 mm thick were evaluated by means of uniaxial tensile tests in order to fit both work-hardening and damage parameters according to the simplified Johnson-Cook model, in which the strain-rate and temperature effects were neglected. The obtained set of damage parameters allowed to define an element removal technique in the ABAQUS/Explicit finite element code to simulate the blanking process used to manufacture the nuclear spacer grids of Inconel 718. Based upon usual process and geometrical tooling parameters, a set of 16 numerical simulations were performed to forecast the sheared edge profile zones and the shearing punch load. From the corresponding predictions, the optimum process and tooling parameters set is defined by punch velocity v = 100 mm/min, tooling clearance C = 0.02 mm, punch rake angle α = 12 degrees and die wall angle β = 3 degrees, which provided 21.5% of burnish, 9.6% of rollover, 68.9% of fracture zones together with a burr height of 3.54 μm. Also, it was verified that the adopted element removal technique must be further investigated in order to better predict the burr formation.

6. ACKNOWLEDGEMENTS

The authors express their sincere thanks to “Indústrias Nucleares do Brasil” (INB) which supplied the Inconel 718 uniaxial tensile specimens. Rafael Oliveira Santos and Marcelo Costa Cardoso acknowledge CAPES for the MSc. (CAPES/Electronuclear program) and PhD. Scholarships, respectively. Luciano Pessanha Moreira acknowledges CNPq and FAPERJ for the financial support from research grants.

7. REFERENCES

Anjos, B. B., Moreira, L. P., 2014. “Experimental and numerical analysis of the lateral cutting of hot rolled strips steel”. In *VIII Congresso Nacional de Engenharia Mecânica*. Uberlândia, Brasil.

ABAQUS user’s manual, 2009. Version 6.9, Dassault Systemes Simulia Corp., Providence, RI, USA.

Alexopoulos, N. D., Argyriou, N., Stergiou, V., Kourkoulis, S. K., 2014. “ Fatigue behavior of Inconel 718 TIG welds”. In *Journal of Materials Engineering and Performance*. Vol. 23. p. 2973-2983.

Boljanovic, V., 2004. *Sheet metal forming processes and die design*, Industrial Press, New York.

Johnson G. R., Cook, W. H., 1985. “Fracture characteristics of three metals subjected to various strains, strain rates, temperatures and pressures”. In *Engineering Fracture Mechanics*, Vol. 21, No.1, p. 31-48.

Kajberg, J., Wikman, B., 2007. “Viscoplastic parameter estimation by high strain-rate experiments and inverse modelling – Speckle measurements and high-speed photography”. In International Journal of Solids and Structures. Vol. 44. p.145-164.

Ko, D. C., Kim, B. M., 2000. “Development of an analytical scheme to predict the need for tool regrinding in shearing process”. In *International of Machine Tools & Manufacture*. Vol. 40, p. 1329-1349.

Lemaitre, J., 1996. *A curse on damage mechanics*, Springer, Berlin, 2nd edition.

Marciniak, J., Ducan, J. L., Hu, S. J., 2002. *Mechanics of sheet metal forming*, London, 2nd edition.

Milani, A. S., Dabboussi, W., Nemes, J. A., Abeyaratne, R. C., 2009. “An improved multi-objective identification of Johnson-Cook material parameters”. In *International Journal of Impact Engineering*. Vol.36. p. 294-302.

Pantalé, O., Bacaria, J. L., Dalverny, O., Rakotomalala, R., Caperaa, S., 2004. “ 2D and 3D numerical models of metal cutting with damage effects”. In *Computer Methods in Applied Mechanics and Engineering*. Vol.193. p. 4383-4399.

Pantalé, O., Gueye, B., 2013. “Influence of constitutive flow law in FEM simulation of radial forming process”. In *Journal of Engineering*. p.1-8.

Poizat, C., Campagne, L., Daridon, L., Ahzi, S., Husson, C., Merle, L., 2005. “Modeling and simulation of thin sheet blanking using damage and rupture criteria”. In *International Journal of Forming Process*, Vol. 8, No.1, p. 29-47.

Uhlmann, E., Gerstenberger, R., Kuhnert, J., 2013. “Cutting simulation with the meshfree finite pointset method”. In *14 th CIRP Conference on Modeling of Machining Operations*. p.391-396.

Uhlmann, E., Schulenburg, M. G., Zettier, R., 2007. “Finite element modeling and cutting simulation of Inconel 718”. In *CIRP Conference on Modeling of Machining Operations*, Vol. 56, No.1, p. 61-64.

Wang, J., Kim, N., Lee, H., 2012. “Ductile fracture in the shearing process of Zircaloy sheet for nuclear fuel spacer grids”. In *Metals and Materials International*, Vol.18, No. 2, p. 303-316.

Wang, X., Huang, C., Zou, B., Liu, H., Zhu, H., Wang, J., 2013. “Dynamic behavior and a modified Johnson-Cook constitutive model of Inconel 718 at high strain rate and elevated temperature”. In *Materials Science & Engineering A*, p. 385-390.

8. RESPONSIBILITY NOTICE

The authors are the only responsible for the printed material included in this paper.